Contrib Mineral Petrol (2003) 144: 449–456
DOI 10.1007/s00410-002-0409-y

Alison Pawley

Chlorite stability in mantle peridotite: the reaction clinochlore+enstatite=forsterite+pyrope+H_2O

Received: 10 May 1999 / Accepted: 12 August 2002 / Published online: 27 September 2002

Abstract Chlorite crystallising in hydrated mantle peridotite is a potential source of water for subduction zone volcanism. The reaction clinochlore + enstatite = forsterite + pyrope + H_2O is the important reaction for defining the stability of chlorite in these rocks. It has been investigated in phase-equilibrium experiments in piston-cylinder and multi-anvil apparatus between 2 and 5 GPa. The reaction has a steep, negative P–T slope at low pressures, with brackets at 860–880 °C at 2.5 GPa, 840–860 °C at 3.0 GPa, and 820–840 °C at 3.5 GPa. The reaction flattens out with increasing pressure to ~5.0 GPa at 650 °C. Chlorite compositions close to the reaction were determined from unit-cell parameters measured using high-resolution synchrotron powder diffraction. These showed a decrease in Al content with increasing pressure along the reaction, consistent with calculations using a previously published thermodynamic data set. The experimental results are consistent with the results of earlier studies on the reaction defining the maximum thermal stability of clinochlore, clinochlore = forsterite + pyrope + spinel + H_2O. They have been used in the derivation of revised thermodynamic data for clinochlore in the latest version of the previously published data set. The new results show that chlorite in subducting slab or overlying mantle wedge could dehydrate below subduction zone volcanoes and be a major source of the water required for melting. However, the dehydration reaction is not sufficiently pressure-dependent to be responsible for the narrow range in depth from the volcanoes to the slab, and chlorite will not be the only hydrous mineral involved.

A. Pawley
Department of Earth Sciences,
University of Manchester,
Oxford Road, Manchester M13 9PL, UK
E-mail: alison.pawley@man.ac.uk

Editorial responsibility: W. Schreyer

Introduction

It is generally accepted that water plays a major role in the genesis of subduction zone magmas because, without it, temperatures would be too low in most subduction zones for melting to occur. The water is incorporated in newly formed oceanic crust by hydrothermal alteration close to oceanic spreading ridges, and then released during subduction in dehydration reactions. The released H_2O rises into the overlying mantle wedge where some may be incorporated in hydrous minerals stable to greater depth than the hydrous minerals in the subducting slab. Dehydration reactions in slab or mantle wedge then provide the water necessary for subduction zone volcanism. Various hydrous minerals may be involved in these dehydration reactions, including amphibole (e.g. Tatsumi 1986; Davies and Stevenson 1992), serpentine (Ulmer and Trommsdorff 1995), and chlorite (Tatsumi 1989).

Chlorite is abundant in low- to medium-grade metamorphic rocks of a variety of compositions, including pelites, mafic and ultramafic rocks. Most chlorite compositions can be represented as clinochlore, $(Mg_5Al)(Si_3Al)O_{10}(OH)_8$, with some substitution of Fe for Mg, and some Tschermak's substitution, $MgSi \Leftrightarrow AlAl$, to either more or less aluminous compositions. Compositions closer to end-member clinochlore become more common as metamorphic grade increases. However, in most rock compositions chlorite reacts to higher-grade minerals at pressures well below the source of subduction zone volcanism. It is only in metamorphosed ultramafic rocks that chlorite persists up to high enough pressures for its dehydration to occur beneath subduction zone volcanoes. Examples of chlorite found in relatively high-grade metamorphosed ultramafic rocks include chlorite peridotite in the Western Gneiss Region, Norway, which formed from the metamorphism of garnet-peridotite in the amphibolite facies (Medaris 1984), and chlorite in peridotite inclusions in kimberlite from the Colorado Plateau, USA (Smith 1979).

The amount of chlorite which can form in peridotite will depend on the Al content of the peridotite, as well as the H_2O content. Tatsumi (1989) has calculated that a hydrous peridotite of composition close to pyrolite, containing chlorite as its only hydrous phase, could contain 23% chlorite. This assumes H_2O saturation and, with ~13 wt% H_2O contained in chlorite, the resulting peridotite contains 2.4 wt% H_2O.

There are two regions in subduction zones where peridotite may be hydrated and so contain chlorite: the subducting slab and the overlying mantle wedge. The subducting slab comprises oceanic crust capping lithospheric mantle. Although the crust is predominantly basaltic in composition, exposures of serpentinised peridotite have been found on the ocean floor (e.g. Cannat 1993). The extent of hydrothermal alteration of the peridotite mantle portion of the slab is unknown. Slab peridotite is likely to be depleted in Al_2O_3 relative to "normal" mantle, as it represents the residue after extraction of the crust. Therefore, the amount of chlorite which could form in hydrated slab peridotite will be less than in overlying mantle wedge which has been hydrated by fluids released from the subducting slab. Tatsumi (1989) proposed that a hydrated peridotite layer containing both amphibole and chlorite is formed by hydration from fluids released from the slab, and is dragged down with the slab until the amphibole and chlorite break down. The released H_2O rises into hotter mantle until a region of the mantle is reached in which the temperature is above the wet solidus, where melting occurs and subduction zone magmas are produced. In this model the chlorite dehydration reaction is from Goto and Tatsumi (1990):

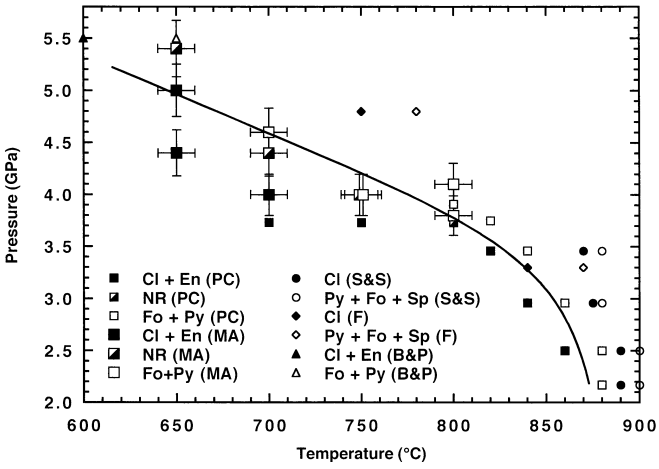

Fig. 1 Results of experiments on reaction (1), clinochlore + enstatite = forsterite + pyrope + vapour. *Small squares* are piston-cylinder experiments (*PC*); *large squares* are multi-anvil experiments (*MA*). Pressure and temperature error *bars* are shown for the multi-anvil experiments; errors on the piston-cylinder experiments are approximately the same size as the *symbols*. Also shown are the results of Staudigel and Schreyer (1977; *S&S*) and Fockenberg (1995; *F*) on reaction (3), clinochlore = forsterite + pyrope + spinel + vapour, and of Bromiley and Pawley (2002; *B&P*) on reaction (1). The *curve* is the position of reaction (1) inferred in this study (see text for further discussion). *Cl* Clinochlore, *En* enstatite, *Fo* forsterite, *Py* pyrope, *Sp* spinel, *NR* no reaction

$$\underset{\text{clinochlore}}{(Mg_5Al)(Si_3Al)O_{10}(OH)_8} + \underset{\text{enstatite}}{2MgSiO_3} = \underset{\text{forsterite}}{2Mg_2SiO_4} + \underset{\text{pyrope}}{Mg_3Al_2Si_3O_{12}} + \underset{\text{vapour}}{H_2O} \quad (1)$$

This reaction is important for defining the stability of chlorite in peridotite saturated in enstatite (orthopyroxene), and within the pyrope (garnet) stability field. The position of the reaction had not been determined experimentally, and so Goto and Tatsumi (1990) estimated it using thermodynamic data available at the time (some measured, some estimated). Given its potential significance in controlling melting in subduction zones, and the uncertainties involved in the thermodynamic calculation, an experimental determination of the reaction is warranted, which will allow more accurate thermodynamic data to be derived. That is the subject of this study.

Previous high-pressure experimental studies on clinochlore

There have been several previous studies of the thermal stability of clinochlore at low pressures, e.g. the reaction

$$\text{clinochlore} = \text{forsterite} + \text{enstatite} + \text{spinel} + H_2O \quad (2)$$

which occurs at $< \sim 2$ GPa (Staudigel and Schreyer 1977; Jenkins 1981; Jenkins and Chernosky 1986). These studies have produced fairly consistent results, although the reaction position obtained by Staudigel and Schreyer (1977) is at a slightly higher pressure than the others. Jenkins (1981) suggests that this is due to an overestimation of pressures by ~9%. There has been less work on the stability of clinochlore at higher pressures. Staudigel and Schreyer (1977) investigated the reaction

$$\text{clinochlore} = \text{forsterite} + \text{pyrope} + \text{spinel} + H_2O \quad (3)$$

up to 3.5 GPa. They located the invariant point where reactions (2) and (3) intersect at 2.03 GPa, 894 °C. Reaction (3) has a steep, negative P–T slope of –930 bar K^{-1} up to 3.5 GPa where the reaction was bracketed at 870–880 °C (Fig. 1). Two brackets on reaction (3) have also been obtained by Fockenberg (1995). They are roughly consistent with the brackets of Staudigel and Schreyer (1977) and indicate that the reaction passes through between 840 and 870 °C at 3.3 GPa, and between 750 and 780 °C at 4.8 GPa (Fig. 1).

Reaction (1) must intersect the same invariant point as located by Staudigel and Schreyer (1977), and also have a negative P–T slope, extending to lower

temperatures at high pressure than reaction (3). A bracket on reaction (1) has recently been obtained in experiments designed principally to investigate the stability of antigorite in the system $MgO–Al_2O_3–SiO_2–H_2O$ (MASH), which used a starting material of aluminous natural antigorite seeded with clinochlore, enstatite, pyrope and forsterite (Bromiley and Pawley 2002). This is also shown in Fig. 1.

Previous studies on chlorite have attempted to determine its composition at its breakdown reactions. Chemical analysis is hindered by fine grain size, and so in most studies X-ray diffraction (XRD) has been used. On the basis of XRD peak positions, Staudigel and Schreyer (1977) inferred that the composition of chlorite at its breakdown reaction (3) is close to pure clinochlore. They did not use a calibration of XRD peak positions, but rather observed no change from their starting material. They based their conclusion also on observed run-product assemblages. Subsequently, Jenkins and Chernosky (1986) synthesised chlorite from three different bulk compositions and derived a calibration of the *c* cell parameter obtained by XRD as a function of Al content. From this they proposed that in fact at the thermal stability limit of chlorite, the stable composition is $(Mg_{4.8}Al_{1.2})(Si_{2.8}Al_{1.2})O_{10}(OH)_8$, with pure clinochlore only being stable below ~700 °C. More recently, Baker and Holland (1996) were able to obtain electron microprobe analyses of three different chlorites, and used these to derive a calibration of unit-cell parameters. They then investigated chlorite compositions as a function of pressure and temperature in reversal experiments. They showed that compositions vary along the univariant chlorite reactions. They also calculated compositions using simple activity-composition models. Their calculations suggest that the Al content of chlorite will decrease with increasing pressure along reaction (1). An activity model for chlorite using their experimental data has been incorporated into the thermodynamic data set of Holland and Powell (1998). This data set can therefore be used to calculate chlorite compositions along reactions. Calculation of reaction (1) using THERMOCALC v3.1 suggests that, between 2 and 5 GPa, the Al content of chlorite decreases by 0.2 p.f.u., from a composition of clinochlore + 0.10 $Al_2Mg_{-1}Si_{-1}$ to one of essentially pure clinochlore. More than half of this decrease occurs between 2 and 3 GPa. These calculated variations will be compared with the experimental compositions obtained in this study.

Experimental technique

Starting materials for the experiments comprised synthetic clinochlore, forsterite, pyrope and enstatite. Mixtures of reagent-grade MgO and Al_2O_3, and SiO_2 glass, in stoichiometric proportions for each phase, were ground under ethanol using an agate pestle and mortar. Clinochlore was synthesised from its oxide mix plus distilled H_2O in a sealed Pt capsule in an internally heated argon pressure vessel at 0.5 GPa, 700 °C, for 48 h. X-ray diffraction (XRD) of the run product showed it to be well-crystalline clinochlore plus a trace of talc + forsterite. The sample was also analysed using scanning electron microscopy (SEM), using a JEOL 6400 scanning electron microscope, operated with a beam current of 15 nA and an accelerating voltage of 15 kV. Standards used were synthetic periclase, synthetic corundum and natural wollastonite for Mg, Al and Si respectively. Crystals were too small (< 1 μm) for analysis of individual grains; therefore, it was necessary to analyse aggregates. This made analysis difficult, and so oxide totals were much lower than the ideal 87% for clinochlore: the average of 10 analyses was 76%. The average chlorite composition obtained was $Mg_{4.71}Al_{2.07}Si_{3.09}O_{10}(OH)_8$. However, this analysis must be considered to have a large uncertainty, considering the analytical difficulties.

Pyrope was produced in two experiments run at 2.5 GPa, 900 °C, for a total of 48 h, with regrinding of the material between experiments. The run product consisted of pyrope plus a trace of enstatite. Enstatite was synthesised in an internally heated argon pressure vessel at 0.5 GPa, 900 °C, for 48 h. The run product contained enstatite plus a trace of quartz. Forsterite (synthesised by S.J. Kohn) was prepared in a 1-atm furnace by sintering at 1,300 °C for several days, regrinding and resintering.

The synthetic minerals were mixed in the correct proportions for reaction (1): 1 clinochlore + 2 enstatite + 2 forsterite + 1 pyrope. Experiments were run using 8–10 mg of this mix plus 0.8–1.0 mg H_2O, sealed in 2-mm-diameter Pt capsules.

Experiments on reaction (1) up to 4 GPa used an end-loaded piston-cylinder apparatus, with half-inch diameter salt cells. Flattened capsules were placed perpendicular to the axial Pt/Pt10Rh thermocouple, separated from the thermocouple tip by a 0.6-mm-thick ruby disk to prevent puncturing of the capsule by the thermocouple tip during the experiment. Experiments 1–10 were run "hot piston-out", for which the sample was overpressurised by 0.1–0.2 GPa while heating, and the excess pressure then bled off. Apparently the initial overpressurisation leads to higher actual pressures than measured, since calibration of pressure against the quartz-coesite data of Bohlen and Boettcher (1982) indicates that these pressures are underestimated by 2%. Experiments 11 onwards were run "hot piston-in", whereby the sample was heated during pressurisation and not overpressurised at any point. Calibration of this procedure indicated that a –2% pressure correction was required for these gauge pressures. Pressures listed in Table 1 are the corrected pressures. The pressure uncertainty is ± 0.05 GPa. Temperature was controlled to ± 1 °C using a Eurotherm controller. The effect of pressure on thermocouple e.m.f. was ignored.

Experiments on reaction (1) at 3.8 GPa and above used a multi-anvil apparatus of the Walker design (Walker et al. 1990; Walker 1991). The anvils were 1-inch tungsten carbide cubes with truncated-edge lengths of 12 mm. The octahedral pressure medium was made of MgO castable ceramic ("old-style" Ceramacast 584, Aremco Products). Graphite furnaces were used (4.2-mm o.d., 3.4-mm i.d.). Temperatures were measured using axial Pt/Pt10Rh thermocouples placed in direct contact with the Pt capsule containing the sample. MgO spacers and insulators were placed around the thermocouple and capsule. Experiments were pressurised cold, and then heated while maintaining constant pressure. Pressures were calibrated at room temperature using the Bi I–II and Bi III–V transitions, and at high temperature using the SiO_2 quartz–coesite and $CaGeO_3$ garnet–perovskite transitions (at 3.0 GPa, 1,000 °C and 6.1 GPa, 1,000 °C respectively; Bohlen and Boettcher 1982; Susaki et al. 1985). The pressure uncertainty (estimated from the calibration experiments) is ± 5%, corresponding to ± 0.2–0.3 GPa. The thermal gradient along the ~2 mm length of sample in the Pt capsule is assumed, on the basis of calibration experiments using two thermocouples (Chinnery 1999), to be no more than 10 °C mm^{-1}.

After the experiments, H_2O saturation was checked by weighing the capsules before and after puncturing. Any capsules which did not lose weight were discarded. Run products were recovered as powders which were examined optically and by XRD. Reaction direction was determined by comparing the XRD patterns of the starting material and the run products. In all experiments equilibration was evidently rapid, since most run products showed strong

Table 1 Results of experiments on the reaction clinochlore + enstatite = forsterite + pyrope + vapour (abbreviations as in Fig. 1)

Experiment No.	Pressure[a] (GPa)	Temperature (°C)	Duration (h)	Run products[b]
Piston-cylinder experiments				
7	2.2	880	22	Fo Py (Cl En)
3	2.5	880	24	Fo Py (Cl En)
1	2.5	860	47	Cl En (Fo Py)
4	3.0	860	24	Fo Py (Cl En)
5	3.0	840	93	Cl En (Py)
8	3.5	840	24	Fo Py (En)
9	3.5	820	25	Cl En (Fo Py)
10	3.7	820	24	Fo Py (En)
11	3.7	800	8	Cl En Fo Py
14	3.9	800	8	Fo Py (En)
18	3.7	750	8	Cl En (Py)
19	3.7	700	8	Cl En (Py)
Multi-anvil experiments				
16	3.8	800	8	Fo Py (En)
15	4.1	800	9	Fo Py (En)
17	4.0	750	10	Fo Py (Cl En)
27	4.0	750	8	Cl En Fo Py
20	4.0	700	9	Cl En (Py)
21	4.4	700	8	Cl En Fo Py
22	4.6	700	8	Fo Py (Cl En)
23	4.4	650	8	Cl En (Py)
25	5.0	650	9	Cl En (Py)
26	5.4	650	8	Cl En Fo Py

[a]Pressure is corrected after applying a +2% correction to experiments up to number 10 (run "hot piston-out"), and a –2% correction to higher number piston-cylinder experiments (run "hot piston-in")

[b]In all experiments where reaction was detected, the reaction was strong, and the phases shown in brackets are present in only minor amounts (except for experiments 4 and 7 where reaction was not as strong but ratios of combined heights of three or four XRD peaks for each phase still changed by > 50%). Where no reaction was detected, no phase is enclosed in brackets

reaction even at temperatures as low as 650 °C and run duration as short as 8 h. In many experiments reaction was strong enough to completely consume one of the starting minerals. Where all four minerals remained in the run product, changes in proportions of XRD peak heights of > 50% readily allowed the determination of reaction direction. In those experiments where no change in mineral proportions was apparent from the XRD patterns, it was assumed that the run conditions were close to the reaction position.

In order to determine the extent of the departure of chlorite compositions from ideal clinochlore, analysis of chlorites from experiments in the clinochlore + enstatite stability field close to reaction (1) was attempted by SEM. However, the chlorites were very fine-grained, occurring mostly as microcrystalline aggregates, with a few thin plates up to ~10 μm diameter, and so analysis was subject to the same problems as for the starting material. Therefore, an alternative means of analysis was sought. As mentioned above, chlorite compositions in the system MASH can be derived from measured unit-cell parameters. However, measurement of unit-cell parameters using conventional XRD proved to be unsatisfactory, as the multi-phase nature of the samples led to significant peak overlap and hence few refinable chlorite peaks, resulting in large errors on the refinements. This problem was overcome by using synchrotron XRD which provided much improved resolution of the chlorite peaks. Thus, the derived unit-cell parameters have uncertainties more than an order of magnitude less than obtained using conventional XRD.

The synchrotron XRD measurements were performed on Station 2.3 (Collins et al. 1992; MacLean et al. 2000) at the Synchrotron Radiation Source, Daresbury Laboratory. A large beam of 1.8×15 mm^2 with $\lambda = 1.39884(1)$ Å was used. The wavelength was calibrated using the first nine peaks of a high-quality silicon powder. Each sample was mounted on a Si(520) single crystal wafer with a diameter of 25 mm. Diffraction data were collected by scanning $\theta/2\theta$ (Hart-Parrish geometry) from $2\theta = 5$ to 60° in steps of 0.01° with 1 s per step. Unit-cell parameters were determined by least-squares refinement, using the programme UNITCELL (Holland and Redfern 1997).

Enstatite compositions were also analysed by SEM to determine the extent, if any, of Al incorporation through the Tschermak's exchange.

Results

Results of experiments on reaction (1) are listed in Table 1 and plotted in Fig. 1. The piston-cylinder experiments provide brackets on reaction (1) which are 20 °C wide up to 3.5 GPa, indicating that at these pressures the reaction has a steep, negative P–T slope. Extrapolation down to 2 GPa shows reasonably good agreement with the results of Staudigel and Schreyer (1977) on reactions (2) and (3). Our results suggest a slightly lower temperature for reaction (1) at 2 GPa than their invariant point (894 °C), but the results agree within error, and agreement is better if a –9% pressure correction is applied to their results, as proposed by Jenkins (1981).

We performed experiments at 800 °C in both apparatus, in order to check consistency between the pressure calibrations. The results are in good agreement, and the lower-temperature piston-cylinder results are also consistent with the multi-anvil results at the same temperatures. However, the multi-anvil experiments at 650, 700 and 750 °C show that the pressure uncertainties on these experiments are large, since the slope of the reaction cannot increase with decreasing temperature (i.e. become more negative). Experiment 27 (4 GPa, 750 °C) was run in order to check the result of experiment 17. It was run for only 8 h, as this duration had been shown in earlier experiments to be sufficient to produce close to 100% reaction. In this case there was no reaction, indicating that the P–T conditions were closer to the equilibrium curve. Thus, the measured pressure in experiment 27 is probably closer to the true pressure than it is in experiment 17. The position of reaction (1) in

Fig. 1 is drawn close to the upper-pressure error limit of experiment 17 so that the reaction position is reasonably consistent with the brackets of Bromiley and Pawley (2002) at 5.5 GPa.

Compositions of run products

Synchrotron powder diffraction was used to measure unit-cell parameters of chlorites from five run products (Table 2). Eleven–seventeen reflections were used in the refinements. Previous studies have shown that c shows the largest variation with composition. Baker and Holland (1996) used their experimental data to derive the relationship c (Å) = 14.642–0.250X_{Chl}, where X_{Chl} is X in the general formula $(Mg_{6-X}Al_X)(Si_{4-X}Al_X)O_{10}(OH)_8$. The data in this study are plotted in Fig. 2, which shows both c and the derived X_{Chl} as a function of pressure, with the run temperatures shown beside each point. It is clear that c increases with increasing pressure (and decreasing temperature) along reaction (1), corresponding to a decrease in Al content from clinochlore + ~0.09 $Al_2Mg_{-1}Si_{-1}$ at 2.5 GPa, 860 °C to clinochlore + ~0.02 $MgSiAl_{-2}$ at 5.0 GPa, 650 °C. These P–T conditions do not lie directly on the reaction but are displaced into the chlorite + enstatite field. Nevertheless, the compositions derived from the unit-cell parameters are in excellent agreement with the calculations using THERMOCALC.

It is worth noting that the unsuccessful SEM analyses also suggested a decrease in X_{Chl} of 0.1 from 3.0 GPa (experiment 5) to 5.0 GPa (experiment 25), but the uncertainties on those values were as large as the variation between them. It is also worth noting that SEM analysis of experiments 5 and 18 (at 3.0 and 3.7 GPa respectively) gave similar compositions to that of the starting material (given in the experimental technique section), suggesting that the latter also has X_{Chl} of ~1.07.

High-temperature orthopyroxenes often contain some Al in the form of a Mg-Tschermak's component. In this study, Al contents of enstatite crystals analysed from the experiments run close to reaction (1), from 3.0 to 5.0 GPa, were all below detection limits. Therefore, the pyroxene can be considered as pure enstatite. Using an ideal mixing model, Holland and Powell's (1998) data set suggests a decrease in Al content from 0.06 to 0 p.f.u. from 3 to 5 GPa.

Discussion

The phase-equilibrium experiments of this study have shown that reaction (1) has a steep negative slope at lower pressures, passing through ~870 °C at 2.5 GPa, with an increasingly shallow slope at higher pressures, such that it passes through ~650 °C at 5.0 GPa. The reaction position which best fits the data is shown in Fig. 3. A curve for reaction (3) can also be drawn, using the data of Staudigel and Schreyer (1977) and Fockenberg (1995). The brackets of these two studies are consistent with each other within experimental uncertainty. Reaction (3) also bends back to low temperatures at high pressure (Fig. 3).

One of the aims of this study was to obtain brackets on reaction (1) which could be used to improve the

Table 2 Unit-cell parameters of chlorites determined by synchrotron powder diffraction. Values in *brackets* are 95% confidence limits

Experiment No.	a (Å)	b (Å)	c (Å)	β (°)	V (Å^3)
1	5.3194(5)	9.2148(7)	14.3694(10)	97.090(7)	698.96(9)
5	5.3200(3)	9.2150(4)	14.3737(5)	97.079(4)	699.28(5)
18	5.3202(27)	9.2183(25)	14.3741(75)	97.067(29)	699.59(34)
20	5.3193(22)	9.2165(23)	14.3802(55)	97.050(22)	699.66(29)
25	5.3204(22)	9.2179(22)	14.3967(57)	97.073(25)	700.69(29)

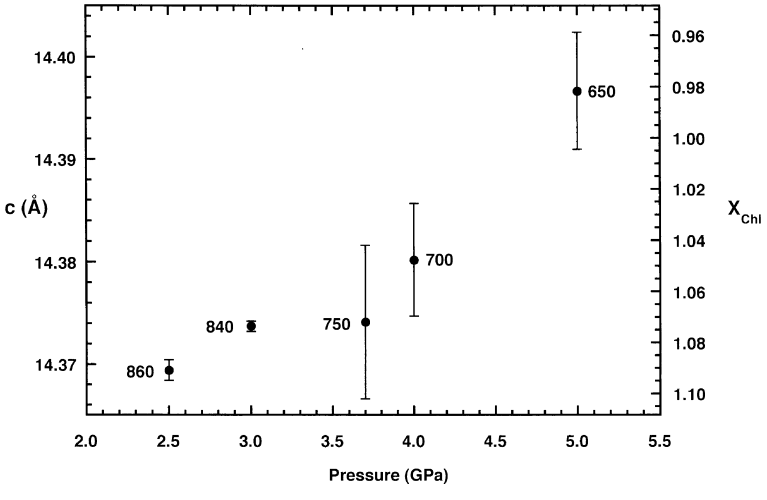

Fig. 2 Unit-cell parameter c of chlorites and corresponding X_{Chl} as a function of pressure along reaction (1). X_{Chl} was derived from the relationship of Baker and Holland (1996). Experimental temperatures are shown beside each data point. *Error bars* indicate 95% confidence limits on c

thermodynamic data for clinochlore used in reaction calculations. Until this study on reaction (1), and that of Fockenberg (1995) on reaction (3), no phase-equilibrium experiments had been done on chlorite reactions above 3.5 GPa. Thus, any calculations of chlorite reactions relevant to, say, dehydration of subducting slab, had to rely on thermodynamic data extracted from lower-pressure studies and extrapolated to higher pressure. Holland and Powell's (1998) data set, which was accompanied by version 2.7 of their computer programme, THERMOCALC, used phase-equilibrium data up to 2.6 GPa (the results of Staudigel and Schreyer (1977) were not used). Calculation of the positions of reactions (1) and (3) using THERMOCALC v2.7 show that there is a problem with the data in that version of the data set. At 2.0 GPa, the experimental reactions are 20–30 °C above their respective calculated reactions, but they cross over to lower temperatures between 3.0 and 3.5 GPa. Both reactions then have a much shallower P–T slope than calculated, such that by 5 GPa the calculated positions are 150 and 130 °C above the experimental positions respectively (these values refer to calculations using fixed clinochlore and enstatite compositions; using variable chlorite and orthopyroxene compositions shifts calculated reaction temperatures by no more than 10 °C). These discrepancies indicate that there is a significant error in one or more of the thermodynamic parameters in THERMOCALC v2.7, which is not evident when only low-pressure reactions are calculated. The strong pressure-dependence of the discrepancies suggests that it is the volume behaviour at high pressure of one or more of the phases which is the culprit. Error in the thermodynamic data for the anhydrous phases involved in the reactions can probably be ruled out, since relatively recent data for these are included in the data set. This leaves only clinochlore and H_2O.

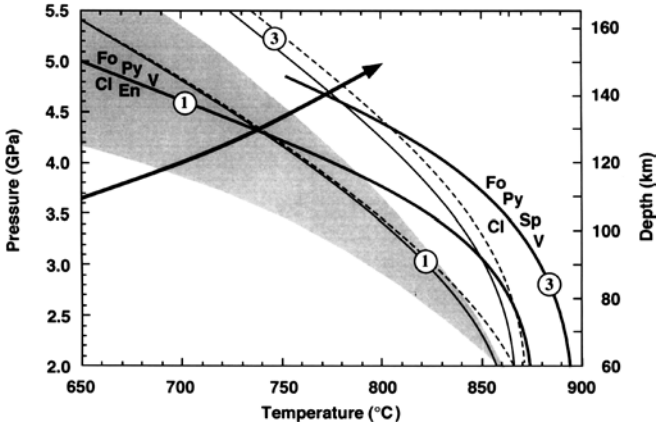

Fig. 3 Experimental and calculated positions of reaction (1), clinochlore + enstatite = forsterite + pyrope + vapour, and reaction (3), clinochlore = forsterite + pyrope + spinel + vapour. Experimental curves (*thick solid lines*) are from Fig. 1 (reaction 1) and from the data of Staudigel and Schreyer (1977) and Fockenberg (1995) (reaction 3). Calculated curves used THERMOCALC v3.1 (Holland and Powell 1998): *thin solid lines* pure phases, *thin broken lines* variable chlorite and orthopyroxene compositions. The *shaded field* shows the range of reaction positions from Goto and Tatsumi (1990): lower-P limit is $\Delta\alpha V = \Delta\beta V = 0$; upper-P limit is $\Delta\alpha V \neq 0$, $\Delta\beta V \neq 0$ (volume data from Holland and Powell 1985). The *arrow* is a P–T path for descending slab from Kincaid and Sacks (1997)

The value of clinochlore's thermal expansivity given in Holland and Powell (1998) and used in THERMOCALC v2.7 is from the measurement by Nelson and Guggenheim (1993) on a sample reasonably close in composition to clinochlore. For compressibility, a bulk modulus of K = 472 kbar was derived from the measurements of Hazen and Finger (1978). Those measurements were made on an Fe- and Al-rich sample significantly different in composition from clinochlore, and only two high-pressure data points were obtained. The data must therefore be treated with suspicion. Recent measurements of the compressibility of close to pure synthetic clinochlore indicate that it is in fact approximately half as compressible as suggested by the data of Hazen and Finger (1978), i.e. K = 869 kbar (Pawley et al. 2002). The new bulk modulus of chlorite has been incorporated into the latest version of THERMOCALC, v3.1 (data set produced on 18 September 1999), along with revised values of enthalpy of formation and entropy of clinochlore. Enthalpies of formation in the data set are derived from least-squares fits of phase-equilibrium data, which in the case of clinochlore now includes the brackets on reaction (1) obtained in this study, and the brackets on reaction (3) obtained by Fockenberg (1995). The enthalpy of formation of chlorite in THERMOCALC v3.1 is –8,313.09 kJ mol^{-1}, as compared to –8,929.86 kJ mol^{-1} in v2.7. The entropy of clinochlore, which is estimated, was raised by 20 J (from 410.5 to 430.5 J K^{-1} mol^{-1}).

The calculated positions of reactions (1) and (3) using THERMOCALC v3.1 are shown in Fig. 3. Reactions are shown both for pure phases and allowing for solid solution in chlorite and orthopyroxene (as described above). These calculated reactions are now in much better agreement with the experiments. However, the degree of curvature of both experimental reactions is still not reproduced by the calculations, suggesting that there is also an error in the EOS of H_2O used in THERMOCALC. In theory, the EOS of H_2O can be tested by comparing experimental and calculated positions of other dehydration reactions which occur in a similar P–T range, for which reliable thermodynamic exist for all of the solid phases involved and the reaction has been well determined experimentally. Unfortunately, there are few such reactions. One useful reaction for comparison is the talc dehydration reaction, talc = enstatite + coesite + H_2O. This was determined by Pawley and Wood (1995) to pass through approximately 810 °C at 3 GPa and 710 °C at 5 GPa. This is again at lower temperatures and with a shallower slope than the reaction calculated using THERMOCALC v3.1, which passes through 825 °C at 3 GPa and 764 °C at 5 GPa. Relatively good thermodynamic data exist for all of the solid phases involved in the reaction. This does suggest

that there is a problem with the EOS of H_2O used in THERMOCALC at these P–T conditions. It is hard, however, to make a rigorous comparison between experimental and calculated reactions on the basis of the present study, as the calculated reaction position is very sensitive to the estimated entropy (such that an increase in entropy of 10 J K^{-1} mol^{-1} has the effect of increasing the reaction temperature by 50–60 °C at 2 GPa).

It is interesting to note that at high pressures the experimentally determined reaction (1) passes between the limits of the calculated reaction of Goto and Tatsumi (1990). The shaded field in Fig. 3 spans those authors' positions of reaction (1) from calculation assuming constant volume change across the reaction (lower-pressure limit) to calculation using volume data from Holland and Powell (1985) (higher-pressure limit). That thermodynamic data set used very simple linear models of thermal expansivity and compressibility, and the former was estimated for clinochlore.

Implications for chlorite stability in subduction zones

Figure 3 shows that the new data obtained in this study are consistent with the dehydration curves used by Tatsumi (1989) in his model of subduction zone magma genesis, in which chlorite in hydrated mantle peridotite could release H_2O directly below subduction zone volcanoes. These volcanoes occur at a narrow range in height above the descending slab (112 ± 19 km depth to the dipping seismic zone for most subduction zones, Tatsumi 1986). Modelling of the thermal structure of subduction zones (e.g. Kincaid and Sacks 1997) indicates that slab P–T paths may intersect reaction (1) at this depth interval. One such path is shown in Fig. 3. It is for a young plate (45 km thick), a slow subduction rate (1.3 cm $year^{-1}$) and dip of 45° (Kincaid and Sacks 1997). Although the position of reaction (1) is fairly sensitive to pressure, Fig. 3 shows that it is not sufficiently pressure-sensitive to account for the narrow range of heights of subduction zone volcanoes above the descending slab, particularly as P–T paths will vary for different subduction rates and angles, and ages of the slab. Therefore, although it will be a good source of water for subduction zone volcanism, there must be another explanation for the location of the volcanoes. Amphibole breakdown has often been cited (e.g. Tatsumi 1986; Davies and Stevenson 1992), but it breaks down at too low a pressure to be directly responsible (e.g. < 2.75 GPa just below the solidus in spinel peridotite, Millhollen et al. 1974). Schmidt and Poli (1998) assessed all of the available experimental data relevant to hydrous phases in both subducting basaltic and ultramafic compositions. They concluded that slab dehydration is continuous down to 150–200 km depth, and so a model for subduction zone melting must depend simply on the thermal structure in the mantle wedge, which determines the location and extent of melting. Chlorite will be a major transporter of water in descending slab and dragged mantle wedge, and may be the only hydrous phase at temperatures above serpentine breakdown, which occurs below 700 °C (Ulmer and Trommsdorff 1995). When it eventually breaks down it will contribute much of the water necessary for subduction zone melting to occur.

Because reaction (1) has a shallow, negative P–T slope at high pressure, it must be close to its intersection with the antigorite (serpentine) stability field at the highest pressures of the experiments in this study. The recent experiments of Bromiley and Pawley (2002) on aluminous antigorite suggest that at ~5.8 GPa, 570 °C there is an invariant point at which reaction (1) intersects the reaction antigorite = forsterite + enstatite + clinochlore + vapour. The latter reaction has a steep, negative P–T slope. At pressures and temperatures below the invariant point, aluminous antigorite is likely to be the main hydrous phase in mantle peridotite. Its reaction to a chlorite-bearing assemblage may be an important mechanism for transferring H_2O to hotter regions within subduction zones.

Acknowledgements Financial support for this study was provided by NERC grant GR3/10308. I would like to thank Chiu Tang for assistance using Station 2.3 at the SRS, Dave Plant for help with SEM, Tim Holland for discussions about THERMOCALC, and Thomas Fockenberg and Stefano Poli for their constructive reviews of the manuscript.

References

Baker J, Holland TJB (1996) Experimental reversals of chlorite compositions in divariant MgO + Al_2O_3 + SiO_2 + H_2O assemblages. Am Mineral 81:676–704

Bohlen SR, Boettcher AL (1982) The quartz = coesite transformation: A precise determination and the effects of other components. J Geophys Res 87:7073–7078

Bromiley GD, Pawley AR (2002) The stability of antigorite in the systems MgO-SiO_2-H_2O (MSH) and MgO-Al_2O_3-SiO_2-H_2O (MASH): the effects of Al^{3+} substitution on high-pressure stability. Am Mineral (in press)

Cannat M (1993) Emplacement of mantle rocks in the seafloor at mid-ocean ridges. J Geophys Res 98:4163–4172

Chinnery NJ (1999) In-situ, high pressure-temperature studies of hydrous minerals in subduction zones. PhD Thesis, University of Manchester

Collins SP, Cernik RJ, Pattison P, Bell AMT, Fitch AN (1992) A 2-circle powder diffractometer for synchrotron radiation on Station 2.3 at the SRS. Rev Sci Instrum 63:1013–1014

Davies JH, Stevenson DJ (1992) Physical model of source region of subduction zone volcanics. J Geophys Res 97:2037–2070

Fockenberg T (1995) New experimental results up to 100 kbar in the system MgO-Al_2O_3-SiO_2-H_2O (MASH): preliminary stability fields of chlorite, chloritoid, staurolite, MgMgAl-pumpellyite, and pyrope. Bochumer Geol Geotech Arb 44:39–44

Goto A, Tatsumi Y (1990) Stability of chlorite in the upper mantle. Am Mineral 75:105–108

Hazen RM, Finger LW (1978) The crystal structures and compressibilities of layer minerals at high pressure. II. Phlogopite and chlorite. Am Mineral 63:293–296

Holland TJB, Powell R (1985) An internally consistent thermodynamic dataset with uncertainties and correlations. 2. Data and results. J Metamorph Geol 3:343–370

Holland TJB, Powell R (1998) An internally consistent thermodynamic data set for phases of petrological interest. J Metamorph Geol 16:309–343

Holland TJB, Redfern SAT (1997) Unit cell refinement from powder diffraction data: The use of regression diagnostics. Mineral Mag 61:65–77

Jenkins DM (1981) Experimental phase relations of hydrous peridotites modelled in the system H_2O-CaO-MgO-Al_2O_3-SiO_2. Contrib Mineral Petrol 77:166–176

Jenkins DM, Chernosky JV (1986) Phase equilibria and crystallographic properties of Mg-chlorite. Am Mineral 71:924–936

Kincaid C, Sacks IS (1997) Thermal and dynamical evolution of the upper mantle in subduction zones. J Geophys Res 102:12295–12315

MacLean EJ, Millington HFF, Neild AA, Tang CC (2000) A versatile diffraction instrument on station 2.3 of the Daresbury laboratory. Materials Sci Forum 321–323:212–217

Medaris LG (1984) A geothermobarometric investigation of garnet peridotites in the Western Gneiss Region of Norway. Contrib Mineral Petrol 87:72–86

Millhollen GL, Irving AJ, Wyllie PJ (1974) Melting interval of peridotite with 5.7 percent water to 30 kilobars. J Geol 82:575–587

Nelson DO, Guggenheim S (1993) Inferred limitations to the oxidation of Fe in chlorite: A high-temperature single-crystal X-ray study. Am Mineral 78:1197–1207

Pawley AR, Wood BJ (1995) The high-pressure stability of talc and 10Å phase: storage sites for H_2O in subduction zones. Am Mineral 80:998–1003

Pawley AR, Clark SM, Chinnery NJ (2002) Equation of state measurements of chlorite, pyrophyllite and talc. Am Mineral 87:1172–1182

Schmidt MW, Poli S (1998) Experimentally based water budgets for dehydrating slabs and consequences for arc magma generation. Earth Planet Sci Lett 163:361–379

Smith D (1979) Hydrous minerals and carbonates in peridotite inclusions from the Green Knobs and Buell Park kimberlitic diatremes on the Colorado Plateau. In: Boyd FR, Meyer HOA (eds) The mantle sample: Inclusions in kimberlites and other volcanics. American Geophysical Union, Washington, DC, pp 345–356

Staudigel H, Schreyer W (1977) The upper thermal stability of clinochlore, $Mg_5Al(AlSi_3O_{10})(OH)_8$, at 10–35 kb P_{H2O}. Contrib Mineral Petrol 61:187–198

Susaki J, Akaogi M, Akimoto S, Shimomura O (1985) Garnet-perovskite transformation in $CaGeO_3$: In situ x-ray measurements using synchrotron radiation. Geophys Res Lett 12: 729–732

Tatsumi Y (1986) Formation of the volcanic front in subduction zones. Geophys Res Lett 13:717–720

Tatsumi Y (1989) Migration of fluid phases and genesis of basalt magmas in subduction zones. J Geophys Res 94:4697–4707

Ulmer P, Trommsdorff V (1995) Serpentine stability to mantle depths and subduction-related magmatism. Science 268:858–861

Walker D (1991) Lubrication, gasketing, and precision in multianvil experiments. Am Mineral 76:1092–1100

Walker D, Carpenter MA, Hitch CM (1990) Some simplifications to multianvil devices for high pressure experiments. Am Mineral 75:1020–1028